Chemical Science

Accepted Manuscript

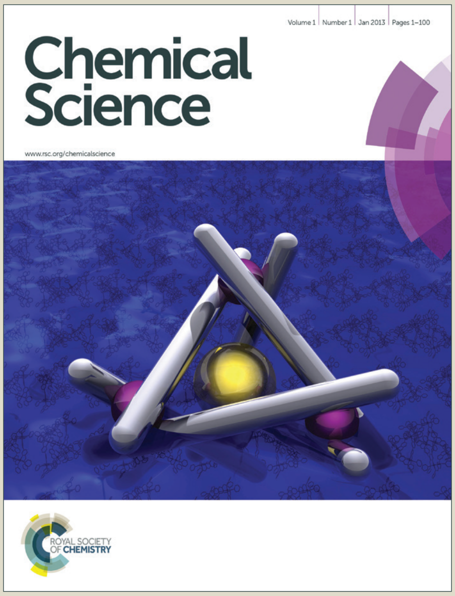

ROYAL SOCIETY OF CHEMISTRY

www.rsc.org/chemicalscience

Chemical Science RSCPublishing

ARTICLE

Pressure stabilization of the long-missing bare C_6 hexagonal rings in the Binary Sesquicarbides

Cite this: DOI: 10.1039/x0xx00000x

Xin Zhong[a,b], Yanchao Wang[a], Feng Peng[a], Hanyu Liu[a], Hui Wang*[a], and Yanming Ma*[a,b]

Received 00th January 2012,
Accepted 00th January 2012

DOI: 10.1039/x0xx00000x

www.rsc.org/

Carbon (C) is able to form various bonding patterns, including graphene sheets, chains, and dimers, but the stable bare six-membered C_6 hexagonal rings as the fundamental structure motifs of graphite and graphene are long missing. We here report the stabilization of such bare C_6 rings under high pressures in the charge-transferred systems of binary sesquicarbides Y_2C_3 and La_2C_3 predicted by the first-principles swarm structure searching simulations. We found that external pressures can efficiently tune structural transitions of sesquicarbides from ambient-pressure cubic phase into high-pressure orthorhombic phases, accompanying by significant C-C bonding modification from C-C dimers in turn to bare C_6 rings and polymerized graphene-like double C_6 sheets. The bare C_6 rings are stabilized in Y_2C_3 and La_2C_3 at pressures above 32 and 13 GPa, respectively, readily accessible to experiments. Chemical bonding analysis reveals that bare C_6 rings feature benzene-like sp^2 C-C bonding patterns with a delocalized π system. The Y or La → C charge transfer and the needs for denser structure packing are found to be the underlying mechanism for the stabilization of bare C_6 rings.

Introduction

C has the ability to form *sp*, *sp*^{2}, and *sp*^{3} bonding and therefore exists in various forms including known structures of graphite, diamond, graphene, fullerenes, nanotubes, etc. Because of the short bond lengths, the 2p orbitals of C can form π bonds, leading to the formation of C patterns of graphene sheets, polymer chains, and dimers.[1, 2] Isolation of one single layer of graphite leads to the stabilization of graphene. Six-membered monocyclic C_6 hexagonal rings (thereafter simplified as “C_6 rings”) as the fundamental structure motifs are interlinked to form graphite and graphene. There, C features typical sp^2 C-C bonding and the rest of unsaturated electrons forms π bonds perpendicular to the layer.

It has been an intense activity to explore C_6 clusters due to the scientific importance of the research in correlation to astrophysics, materials science and combustion processes.[3, 4] The first theoretical investigation on C_6 clusters was traced back to 1959.[5] A C_6 ring has energy close to the triplet cumulenic state but exists in an energetically unfavorable geometry of a saddle point.[6] A linear chain form of C_6 cluster is found to be more stable than the (distorted) C_6 ring structure[7]. As a consequence, only the linear chain form of C_6 cluster has been experimentally synthesized.[8, 9] The searching of bare C_6 ring in isolated clusters failed. Gas phases of positively charged linear and cyclic C_6^+ were generated in hot cathode-discharge ion sources from perchloro- or perbromobenzene (e.g., Refs. 10-11). However, these gas C_6 cations are energetically unfavorable and they are reactive intermediate, which can only be recorded in neon matrices at rather low temperature (e.g., 6 K).

Formation of bare C_6 rings in bulk crystal is also yet established. Chemically, bare C_6 rings are unfavorable due to the existence of unsaturated electrons per C. Benzene (C_6H_6), cyclohexane (C_6H_{12}) and the recently proposed SiC_3[12] compounds contain such a backbone of C_6 ring, but each C has to bond with external hydrogen or silicon to achieve the stable state of an 8e-closed electron shell of C. Extra electrons are apparently needed to stabilize bare C_6 rings. This motivates us to pursue bare C_6 rings in systems that C is capable of acquiring exotic electrons.

Results and discussion

In an effort to stabilize the bare C_6 rings, we focus on the charge-transferred systems of binary sesquicarbides R_2C_3 (R= Y and La), where the rare-earth metals donate electrons to C.

R_2C_3 crystallizes in a cubic Pu_2C_3-type structure at ambient pressure (space group *I*-43*d*, denoted as α-structure/phase), where C atoms form doubly bonded C-C dimers.[13, 14] These R_2C_3 systems have been extensively studied to understand their peculiar superconductivities[15-17] at ambient pressure.

We here tune the phase structures of R_2C_3 by external high pressures through swarm-intelligence CALYPSO structure searching techniques[18, 19] unbiased by any prior known structure knowledge in conjunction with first-principles density functional calculations. For the first time, bare C_6 rings were successfully stabilized in the high-pressure orthorhombic phases of Y_2C_3 and La_2C_3 above pressures of 32 GPa and 13 GPa, respectively, accessible to the high-pressure experiments.

We searched the structures of Y_2C_3 and La_2C_3 with simulation cell sizes of 1 - 4 formula units (f.u.) in the pressure range 0 - 300 GPa through CALYPSO code.[18, 19] The effectiveness of our structure searching method has been demonstrated by recent successes in correctly predicting high-pressure structures of various compounds.[20-22] The local structural relaxations and electronic band structure calculations were performed in the framework of density functional theory within the generalized gradient approximation and frozen-core all-electron projector-augmented wave (PAW) method[23, 24] as implemented in the VASP code.[25] The PAW potentials for Y、La and C were taken from the VASP library where $4s^24p^65s^24d^1$、$5s^25p^65d^16s^2$ and $2s^22p^2$ electrons were used as valence electrons for Y、La and C, respectively. The cutoff energy of 800 eV and appropriate Monkhorst-Pack (MP)[26] *k* meshes were chosen to ensure that all the enthalpy calculations were well converged to 1 meV/ atom. We also calculated the atomic- and molecular-orbital energy levels of the C_2 dimer and C_6 ring through Amsterdam Density Functional (ADF) program,[27] The phonon calculations have been carried out by using a supercell approach as implemented in the PHONOPY code.[28] Electron-phonon coupling calculations have been performed using the pseudopotential plane-wave method and density-functional perturbation theory[29, 30] as implemented in the QUANTUM ESPRESSO package.[31] A 2 × 2 × 2 MP *q*-point mesh was used and a 6 × 6 × 6 MP *k* mesh is chosen to ensure *k*-point sampling convergence with Gaussians of 0.05 Ry, which approximates the zero-width limit.

Our structure searching simulations on Y_2C_3 performed at 0 and 30 GPa with the input information of chemical compositions of Y : C = 2 : 3 readily reproduced the experimental α-structure (Figure 1A). This proved the reliability of our method in application to this sesquicarbide system. This α-phase features the doubly bonded C-C dimer with a bondlength of 1.338 Å at ambient pressure. At elevated pressures of 50 and 100 GPa, our structure simulations uncovered a peculiar orthorhombic phase (space group *Fmmm*, Z = 8, denoted as β-phase, Figure 1B and C). In this structure, C atoms form the long-missing bare C_6 ring. The C-C bond lengths are nearly perfectly equal (four bond lengths at 1.51 Å and two bond lengths at 1.50 Å at 50 GPa). The C-C distance between the nearest-neighboring C_6 rings is fairly large (3.41 Å at 50 GPa), excluding from any bonding possibility between the C_6 rings. There are two kinds of Y atoms. One kind locates right above and below the center of C_6 rings, and two such Y atoms together with one C_6 ring form dodecahedron [Figure 1C]. The other kind of Y atoms sits in the interstitial space of the dodecahedrons. [Further structural information can be seen in the Supplementary Table S1]

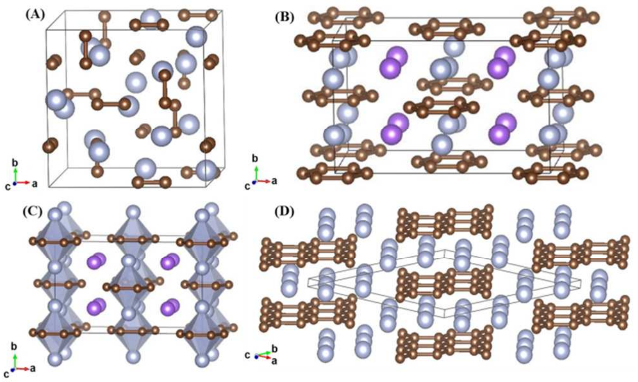

Figure 1 (Color online). (A) and (D) depict crystal structures of α- and γ-Y_2C_3. (B) and (C) are two different illustrations of β-Y_2C_3 structure. The small and large spheres represent C and Y atoms, respectively. Atoms in blue and purple represent two different kinds of Y atoms, respectively.

At 200 and 300 GPa, our structure searching calculations unraveled another orthorhombic phase (space group *Cmcm,* denoted as γ-phase, Figure 1D). This structure can be viewed as the polymerized structure of C_6 rings and possesses intriguing sheet patterns. The sheet has a width of double C_6, but is infinite long along *c* axis. This C structure moiety might be seen as the smallest graphene-like pattern.

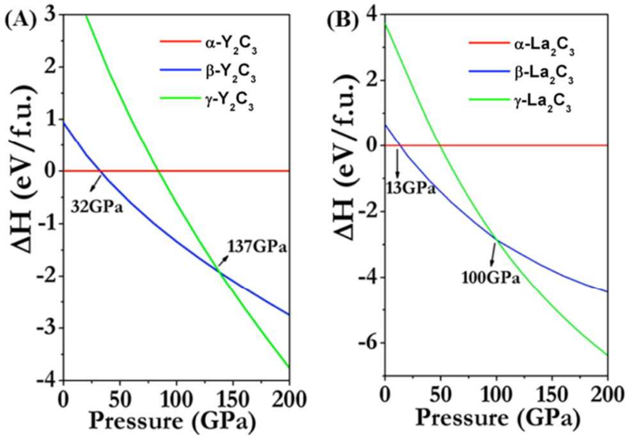

Figure 2 (A) and (B) enthalpy curves of β- and γ-phases (relative to the α-phase) as a function of pressure for Y_2C_3 and La_2C_3, respectively.

Enthalpy curves (relative to α-phase) as a function of pressure for these two predicted β- and γ-phases of Y_2C_3 are presented in Figure 2A. It is clearly seen that the ambient-pressure α-phase is stable up to 32 GPa, above which β-phase becomes more favorable. γ-phase surpasses β-phase above 137 GPa. Extensive structure searching simulations for La_2C_3 were also performed at 40 GPa and 110 GPa and the same existence of high-pressure β- and γ- structures in La_2C_3 was confirmed. The α → β transition pressure of La_2C_3 at 13 GPa is apparently lower than that in Y_2C_3 (Figure 2B). Phonon calculations using the supercell method[30] were performed for β-Y_2C_3 at 50 GPa and γ-Y_2C_3 at 160 GPa to examine the dynamical stabilities of the two structures. The absence of any imaginary phonons in the whole Brillouin zone confirmed their structural stabilities [Supplementary Figure S1].

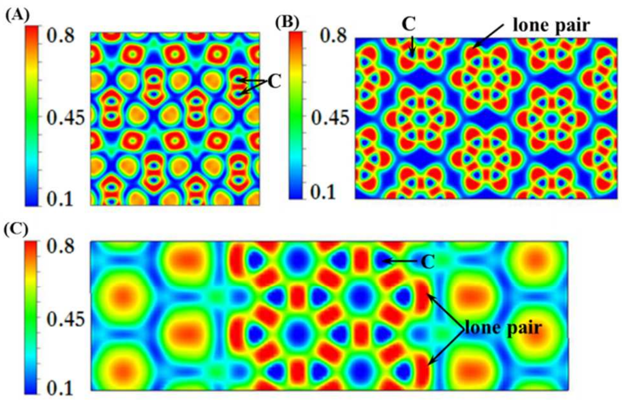

Figure 3. (A)-(C) ELF plots in (001) section for α-, β-, and γ-Y_2C_3 structures, respectively.

In order to probe the C-C bonding nature of α-, β- and γ-Y_2C_3, we have performed chemical bonding analyses through calculations of the electron localization function (ELF).[32] The calculated ELF isosurface for α-Y_2C_3 structure shows that two C atoms bond together to form the doubly bonded C_2 dimer (Figure 3A). In β-Y_2C_3 structure (Figure 3B), it is seen that each C possesses one lone pair of electrons and forms two C-C covalent bonds, and the rest (6 in total) of $2p_z$ electrons of the C_6 rings forms the delocalized π system (supplementary Figure S4). This allows us to identify the sp^2-like C-C bonding nature of β-Y_2C_3. This bonding mechanism resembles with that of benzene, but in contrasted to that (sp^3 hybridization) of cyclohexane. In Figure 3C, the graphene-like sheet in γ-phase features also sp^2 C-C bonding with each inner C atom forming three C-C covalent bonds whilst each outer C atom having one electron lone pair and two C-C covalent bonds.

C atoms must have accepted electrons from Y atoms in order to have the sp^2-bonding orbitals populated. We therefore explicitly calculated the Bader charges of C and Y atoms for various phases as listed in Table 1. At ambient pressure, the Bader charge of C in α-Y_2C_3 phase is about 5.08*e* (*i.e.* each C atom accepts 1.08 electrons from Y atom), which corresponds to the electron loss of 1.63*e* per Y atom. At phase transition into β-Y_2C_3, the charge transfer was slightly depressed with the electron gain of C at approximate 0.96*e* per C.

Table 1 Calculated Bader charges of Y and C atoms in α-, β-, and γ- Y_2C_3.

	Pressure (GPa)	Atoms	Charge value(e)	δ(e)
α-Y_2C_3	0	Y	9.37	+1.63
		C	5.08	-1.08
β- Y_2C_3	50	Y	9.56	+1.44
		C	4.96	-0.96
γ-Y_2C_3	160	Y	10.01	+0.99
		C	4.66	-0.66

δ is the charge transfer from Y to C atom

The C-2*s* and C-2*p* states in β-Y_2C_3 strongly hybridize and reside in the deep level of -11.4~-10.1eV (Supplementary Figure S2). This is associated with the strong sp^2 C-C σ bonding in the C_6 ring. Y-4*d* electron has a dominant contribution to the total density of states at the Fermi Level, but does not participate in the localized bonding. Experimentally, [17] it was observed that α-Y_2C_3 is a superconductor with a transition temperature of 6 K at ambient pressure, in a good agreement with our theoretical calculation of 12 K based on the linear response theory [see Supplementary Information for more computational details]. The same method was applied to explore the possible superconductivity of β-Y_2C_3 at 50 GPa. The obtained electron-phonon coupling parameter λ is 0.28, substantially smaller than that (0.74) of α-Y_2C_3 at zero pressure. Such a small λ doesn't support the superconductivity of β-Y_2C_3.

It is of fundamental interest to understand the underlying mechanism for the stabilization of β-Y_2C_3 structure and thus the bare C_6 rings. Two important aspects should be addressed. First, from the orbital energy levels of molecular C_2 dimer,[33] there is one unpopulated 1 π_u bonding orbital per C_2 dimer ready for acceptance of two extra electrons (Figure 4A). As the consequence of Y→C charge transfer, each C accepts exotic 1.08 electrons from Y to fill up 1 π_u bonding orbital. For the β-Y_2C_3 structure predicted here, there are three unpopulated bonding orbitals ($5B3_u$*, $6A_g$*, and $3B2_g$*) per C_6 ring (Figure 4B) able to accommodate 6e without destabilizing the rings. Since each C accepts about 0.96*e*, anti-bonding orbitals of C_6 ring remained unpopulated. Chemically, C_6 ring remains rather stable. Second, there is a need for denser structure packing under high pressure. As is known that Gibbs free energy reduces to enthalpy H = U + PV at 0 K, where U, P and V are the static energy, pressure and volume per formula unit, respectively. The high-pressure competition between U and PV dominate the phase transitions. Our calculations show that the sphere packing efficiency at 32 GPa increases from 6.25 % in α-Y_2C_3 to 10.05 % in β-Y_2C_3. Obviously, β-Y_2C_3 is more densely packed than that of α-Y_2C_3 at this pressure. As a result, the first order transition of α → β-Y_2C_3 leads to a volume drop of 6.5 % (Supplementary Figure S3A). This volume reduction is critical to initiate the phase transition into β-Y_2C_3 and thus for the stabilization of C_6 rings.

In our studied Y_2C_3 compound, C atom accepts about one electron, and thus is isoelectronic to N. There is a great interest to compare the current finding with that known in the charge transferred system of alkali metal azides[34, 35]. Though N in LiN_3 adopts a linear N-N-N bonding pattern at ambient pressure, recent studies predicted the pressure-induced formation of bare "N_6" rings above 34.7 GPa[34, 35], similar to our findings of C_6 rings. However, below we show that the seemingly similar N_6 and C_6 rings are fundamentally different.

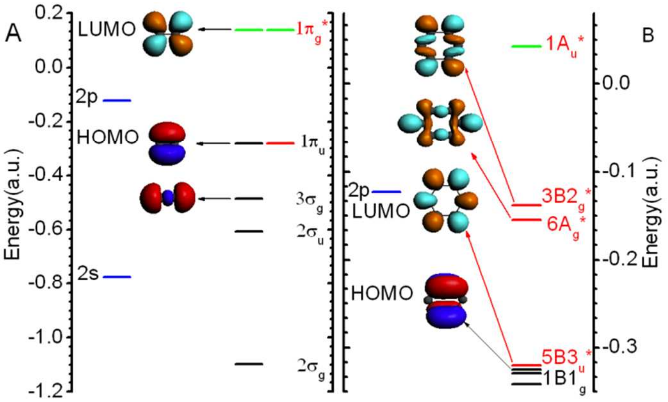

Figure 4. Schematic atomic- and molecular-orbital energy diagrams of C_2 dimer (A) and C_6 ring (B). For each figure, left and right scales are energy levels for atomic and molecular orbitals, respectively. Inset figures explicitly depict the HOMO and LUMO molecular orbitals. Red and black solid lines present the empty and filled molecular orbitals, respectively. In (A), there is one unpopulated $1\pi_u$ bonding orbital ready for acceptance of two extra electrons. Acceptance of more than two electrons will lead to the population of antibonding states of $1\pi_g$* shown in green. In (B), there are three unpopulated bonding orbitals ($5B3_u^*$, $6A_g^*$, and $3B2_g^*$) ready for acceptance of six extra electrons.

In the N_6-ring structure of LiN_3, there is obvious electron depletion of Li, but the electron acceptor is not N atom as inferred from the difference charge density plot (Supplementary Figure S4), where no electron gain in N was found. The depleted charge of Li must have transferred to the interstitial region. Since N does not accept any electron, N_6 ring is isoelectronic to the current C_6^{6-} ring predicted. However, the bonding behavior in N_6 ring is rather different with that in our bare C_6^{6-} ring since there is apparently lack of delocalized π bonding in N_6 ring. Rather, a covalent bonding was evident between inter-layer N_6 rings (Supplementary Figure S4).

We extended our searching of C_6 rings into other rare-earth metal carbides R_2C_3 systems (R = Sc, Lu, Nd, Eu, and Gd) through density functional total-energy calculations (Supplementary Figure S5). Our results showed that C_6 rings could also be stabilized in these compounds. Attempts were also made on actinide carbides (e.g., Pu_2C_3 in Figure S5) and the results supported the similar high-pressure formation of C_6 rings. Stabilization of C_6 rings at high pressures can therefore be regarded as a general behavior for rare-earth metal carbides and actinide carbides. We emphasize that the particular stoichiometry of R:C = 2:3 is rather important in the formation of the dodecahedron structure motifs and thus the C_6 rings. Indeed, C_6 rings are not seen in the high-pressure phases of CaC_2[36], where the compound has also a C-C dimer structure with accepting ca. one electron per C at ambient pressure.

Conclusions

In brief, in searching for the bare C_6 rings, we have performed extensive studies on the high-pressure structures of the charge-transferred systems of sesquicarbides based on the swarm-intelligence structure simulations. Our research highlights the key role of pressure played in the stabilization of the long-missing bare C_6 rings. The underlying mechanisms on the stabilization of C_6 rings have been rationalized by the charge transfer and the needs for denser structure packing. Further total energy calculations extended the C_6 searching from Y_2C_3 and La_2C_3 into entire rare-earth metal carbides and actinide carbides. We found that the stoichiometry ratio of R:C = 2:3 is rather important for the formation of C_6 rings. Our current findings represent a key step forward in the understanding of the behavior of C_6 bonding patterns at high pressures.

Acknowledgements

This research is supported by the China 973 Program (2011CB808200), Natural Science Foundation of China under 11274136, 11104104, 11025418 and 91022029, 2012 Changjiang Scholars Program of China, Changjiang Scholar and Innovative Research Team in University (IRT1132).

Notes and references

[a]State Key Laboratory of Superhard Materials, Jilin University, Changchun 130012, China.
[b]Beijing Computational Science Research Center, Beijing 10084, China.
huiwang@jlu.edu.cn (Hui Wang);
mym@jlu.edu.cn (Yanming Ma)

1 M. J. Rice, A. R. Bishop and D. K. Campbell, *Physical Review Letters*, 1983, **51**, 2136-2139.
2 R. Hoffmann, C. Janiak and C. Kollmar, *Macromolecules*, 1991, **24**, 3725-3746.
3 W. Weltner, Jr. and R. J. V. Zee, Chem.Rev, 1989, **89**, 1713-1714.
4 A. V. Orden and R. J. Saykally, Chem. Rev, 1998, **98**, 2313-2357.
5 K. S. Pitzer and E. Clementi, J. Am. Chern. Soc, 1959, **81**, 4477-4485.
6 K. Raghavachari, R. A. Whiteside and J. A. Pople, J. Chern. Phys. , 1986, **85**, 6623-6628.
7 V. Parasuk and J. Almlof, J. Chern. Phys., 1989, **91**, 1137-1141.
8 R. J. V. Zee, R. F. Ferrante, K. J. Zeringue, W. Weltner and D. W. Ewing, J Phys Chem C, 1988, 88, 3465.
9 H. J. Hwanga, A. V. Ordena, K. Tanakaa, E. W. Kuoa, J. R. Heatha and R. J. Saykallya, Molecular Physics 1993, **79**, 769-776.

10 J. Fulara, E. Riaplov, A. Batalov, I. Shnitko and J. P. Maier, J.Chem.phys, 2004, **120**, 7520-7525.

11 X. Chen, M. Steglich, V. Gupta, C. A. Rice and J. P. Maier, Physical Chemistry Chemical Physics, 2014, **16**, 1161-1165

12 G. Gao, N. W. Ashcroft and R. Hoffmann, J. Am. Chem. Soc., 2013, **135**, 11651-11656.

13 V. I. Novokshonov, Russ. J. Inorg. Chem, 1980, **25**, 375.

14 X. Wang, I. Loa, K. Syassen, R. K. Kremer, A. Simon, M. Hanfland and K. Ahn, Phys. Rev. B, 2005, **72**, 064520.

15 M. C. Krupka, A. L. Giorgi, N. H. Krikorian and E. G. Szklarz, J. Less-Common Met, 1961, **17**, 91-98.

16 B. Cort, G. R. Stewart and A. L. Giorgi, J. Low Temp. Phys., 1984, **54**, 149-154.

17 G. Amano, S. Akutagawa, T. Muranaka, Y. Zenitani and J. Akimitsu, J. Phys. Soc. Jpn., 2004, **73**, 530-532.

18 Y. Wang, J. Lv, L. Zhu and Y. Ma, Physical Review B, 2010, **82**, 094116.

19 Y. Wang, J. Lv, L. Zhu and Y. Ma, Computer Physics Communications, 2012, **183**, 2063-2070.

20 J. Lv, Y. Wang, L. Zhu and Y. Ma, Physical Review Letters, 2011, **106**, 015503.

21 L. Zhu, H. Wang, Y. Wang, J. Lv, Y. Ma, Q. Cui, Y. Ma and G. Zou, Physical Review Letters, 2011, **106**, 145501.

22 Y. Wang, H. Liu, J. Lv, L. Zhu, H. Wang and Y. Ma, Nature Communications, 2011, **2**, 563.

23 P. E. Blöchl, Phys. Rev. B, 1994, **50**, 17953-17979.

24 G. Kresse and D. Joubert, Phys. Rev. B, 1999, **59**, 1758.

25 G. Kresse and J. Furthmüller, Phys. Rev. B, 1996, **54**, 11169-11186.

26 H. J. Monkhorst and J. D. Pack, Phys. Rev. B, 1976, **13**, 5188-5192.

27 G. te Velde, F. M. Bickelhaupt, E. J. Baerends, C. Fonseca Guerra, S. J. A. van Gisbergen, J. G. Snijders and T. Ziegler, J. Comput. Chem., 2001, **22**, 931-967

28 A. Togo, F. Oba and I. Tanaka, Physical Review B, 2008, **78**, 134106.

29 S. Baroni, P. Giannozzi and A. Testa, Physical Review Letters, 1987, **58**, 1861-1864.

30 P. Giannozzi, S. de Gironcoli, P. Pavone and S. Baroni, Physical Review B, 1991, **43**, 7231-7242.

31 A. D. C. S. Baroni, S. d. Gironcoli, P. Giannozzi, C. Cavazzoni, G. Ballabio, S. Scandolo, G. Chiarotti, P. Focher, A. Pasquarello, K. Laasonen, A. Trave, R. Car, N. Marzari and A.Kokalj, http://www.pwscf.org.

32 P.-D. A. Savin, P. D. R. Nesper, D. S. Wengert and D. T. F. Fässler, Angewandte Chemie International Edition in English, 1997, **36**, 1808-1832.

33 K. Raghavachari, R. A. Whiteside and J. A. Pople, J. Chern. Phys. , 1986, **85**, 6623-6629.

34 M. Zhang, H. Yan, Q. Wei, H. Wang and Z. Wu, Europhysics Letters, 2013, **101**, 26004.

35 D. L. V. K. Prasad, N. W. Ashcroft and R. Hoffmann, J Phys Chem C, 2013, **117**, 20838.

36 Y. Li, W. Luo, Z. Zeng, H. Lin, H.-K. Mao and R. Ahuja, Proc. Natl. Acad. Sci. U.S.A., 2013, **110**, 9289-9294.